

Boolean Variation and Boolean Logic BackPropagation

A MATHEMATICAL PRINCIPLE OF BOOLEAN LOGIC DEEP LEARNING

Van Minh Nguyen

Intelligent Computing and Communication Research

Advanced Wireless Technology Laboratory

Paris Research Center, Huawei Technologies

vanminh.nguyen@huawei.com

May 8, 2024

Abstract

The notion of variation is introduced for the Boolean set and based on which Boolean logic backpropagation principle is developed. Using this concept, deep models can be built with weights and activations being Boolean numbers and operated with Boolean logic instead of real arithmetic. In particular, Boolean deep models can be trained directly in the Boolean domain without latent weights. No gradient but logic is synthesized and backpropagated through layers.

1 Introduction

Deep learning has become a commonplace solution to numerous modern problems, occupying a central spot of today's technological and social attention. The recipe of its power is the combining effect of unprecedented large dimensions and learning process based on gradient backpropagation [LeCun et al., 1998]. In particular, thanks to the simplicity of neuron model that is decomposed into a weighted linear sum followed by a non-linear activation function, the gradient of weights is solely determined by their respective input without involving cross-parameter dependency. Hence, in terms of computational process, gradient backpropagation is automated by gradient chain rule and only requires a buffering of the forward input data.

However, deep learning is computationally intensive. Fig. 1 shows its typical operations where the forward pass is used in both inference and training while the backpropagation is only for the training. In inference, the whole model parameters must be stored and the main computation is tensor-dot products. In training, the forward pass, in addition to that of the inference, needs to buffer all input tensors of every layer. They are used for tensor-dot products required by the derivative computation, gradient-descent-based optimizer, and gradient backpropagation. Also required by the gradient-based learning principle, model parameters and all signals are continuous numbers that are typically represented in 32-bit floating-point format. It results in large memory footprint. Fig. 2 shows our one example to illustrate the memory footprint of

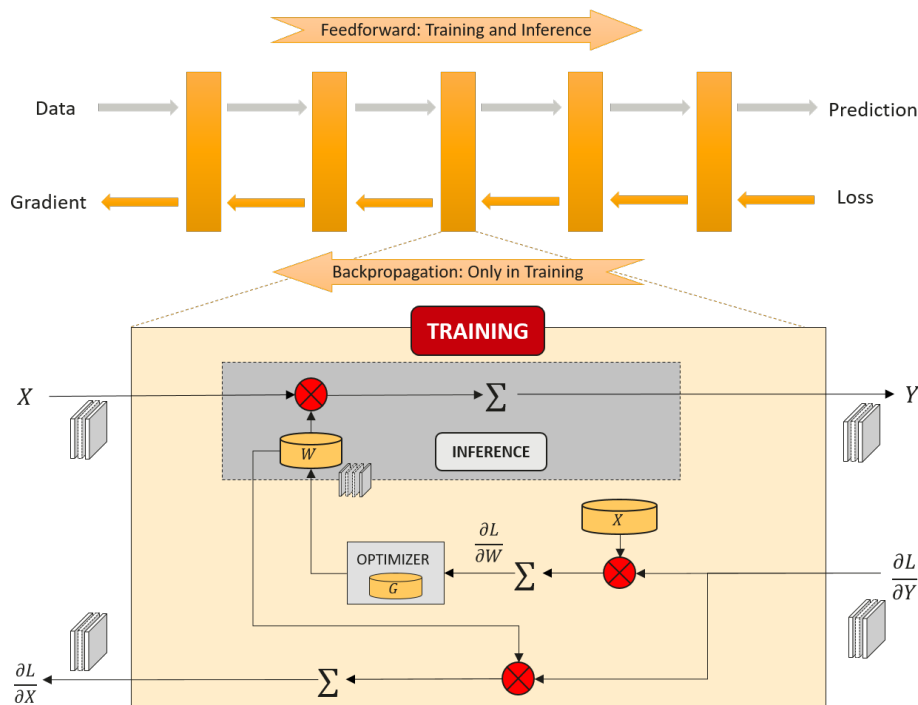


Figure 1: Overview of inference and training processes.

CIFAR-10 classification with VGG-small [Simonyan and Zisserman, 2014]. This model requires 56 MB for parameters whereas its training with stochastic gradient descent and batch size of 100 requires 2 GB for training data and buffers, corresponding to 97% of the total memory requirement. This is known as *memory wall* problem [Liao et al., 2021]. On the other hand, it is intensive in energy consumption due to large amount of floating-point multiplications. On top of that, not only one training process is repeated for a large number (millions) of forward-backpropagation iterations, but also the number of training experiments increases exponentially with the number of hyper-parameters for tuning. [Strubell et al., 2019] showed that the CO2 footprint of training a natural language processing model is above 2000 times more than that of the inference. This problem has motivated a large body of literature that is summarized in Section 2. In particular, there has been motivations to develop *binary neural networks* in which all parameters and/or data are binary numbers requiring only 1 bit. That would bring multiple benefits, notably significant reductions of memory footprint and of data movement and compute energy consumption. This line of research can be summarized into two approaches.

The first one is called network binarization that is based on the existing gradient backpropagation for network training and aims at obtaining a binarized model for inference. This concept was proposed as BinaryConnect by [Courbariaux et al., 2015], Binarized neural networks (BNNs) by [Hubara et al., 2016], and XNOR-Net by [Rastegari et al., 2016]. In BinaryConnect and BNNs, binary weights are obtained by sign extraction from the continuous ones during the continuous network training. In XNOR-Net, activations are real number and weights are binary. It also trains the continuous model by the standard gradient descent; then approximates the obtained continuous weights

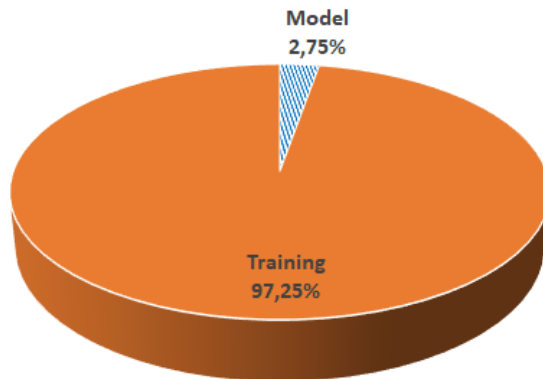


Figure 2: Memory consumption of VGG-small model in 32-bit floating point and batch size of 100 samples for CIFAR10 classification.

by binary weights with a scaling factor subjected to minimizing approximation error. Binarization approach in its core concept can perform relatively well in small tasks such as MNIST and CIFAR-10 classifications, but becomes hard to achieve comparable performance to the continuous model in more challenging tasks. Numerous architecture tweaks have been proposed, e.g., Bethge et al. [2019], Liu et al. [2018, 2020], Zhang et al. [2022b], Guo et al. [2022], aimed at bridging the gap to the continuous model in ImageNet classification. However, it is not clear how such architecture tweaks can be generalized to other computer vision tasks. On the other hand, network binarization is essentially a special case of quantization-aware training when the quantization function is the sign function. Its training is fully based on gradient backpropagation with continuous latent weights that are updated through the classic gradient descent. The derivative w.r.t. the quantized (or binarized) weights is not properly defined and needs to be approximated by a differential proxy. In Hubara et al. [2017], the authors also showed that training a neural network with low-precision weights (even a single-layer one) is an NP-hard optimization problem. Due to weight discretization, the backpropagation algorithm used in continuous model training cannot be used effectively. The problem of unstable gradients appears as soon as the number of bits for representing numbers is less than 8. Through experiment study, Helweggen et al. [2019] observed that the role of latent weights in binarization process seems ignorable.

The second approach aims to train binary neural networks by another principle than the gradient backpropagation. To the best of our knowledge, Expectation Backpropagation [Soudry et al., 2014] was among the first attempts in this direction. It characterizes each weight by a probability distribution which is updated during the training. The network is then specified by sampling weights from the given distributions. Procedures along these lines operate on full-precision training. [Baldassi, 2009] and [Baldassi and Braunstein, 2015] proposed training algorithms inspired from statistical physics that keep and update an integer latent weight for every binary weight. It has been illustrated that these integer latent weights can also have bounded magnitude. This feature greatly reduces the complexity of operations. However, these algorithms are designed for specific types of networks and cannot be applied in a straightforward manner to DNNs and deep architectures. [Baldassi et al., 2015] provides an efficient algorithm based on belief propagation, but as in the previous works, this applies to a

single perceptron and it is unclear how to use it for networks with multiple layers. An alternative approach to overcome the lack of gradient information is to address training as a combinatorial optimization problem and apply a known method for this kind of problems. Evolutionary Algorithms have been proposed as a training method for NNs in general by [Morse and Stanley, 2016], and for low-precision DNNs by [Ito and Saito, 2010]. However, evolutionary algorithms suffer from performance and scalability issues. First, although only low-precision weights are considered, the number of weights stored in memory is multiplied by the population size, and therefore, even for binary weights and a modest population size of 100, the memory footprint is larger than storing decimal weights with 16, 32 or 64 bits floating-point format. Second, a single forward pass during training has to be performed for all members of the population. Even though this can be done in parallel, having as many parallel processors as the population size is practically prohibitive. It is also well known that the population size should increase with the number of weights (dimension of the optimization parameter space), making scaling for big neural networks problematic.

The state of the art as described above shows that it appears possible to constraint deep neural networks to binary weights and/or activation, however how to reliably train binary deep models directly in binary domain remains an open question. This paper presents our attempt to provide a method to this question. Instead of formulating a kind of Boolean derivative such as one by Akers [1959], we introduce the notion of Boolean variation. Then, we develop a method by which one can synthesize logic rules for optimizing Boolean weights as well as ones to be backpropagated during the training phase.

2 Related Works

Beside the most related works that are discussed in the introduction, this section provides a broader view of the literature that deals with the computational complexity of deep learning. It can be categorized into four approaches corresponding to four sources of complexity: large dimensions, intensive arithmetic, data bitwidth, and computing bottleneck.

Based on the fact that deep models are over-parameterized, low-rank factorization exploits this sparsity by means of tensor decomposition such as principal component analysis so as to only keep some most informative parts of the model. Several methods have been proposed in this direction known as compression and pruning [Han et al., 2015, Cheng et al., 2020, Yang et al., 2017b], or network design [Sze et al., 2017, Howard et al., 2017, Tan and Le, 2019]. Besides, knowledge distillation is also an important approach that trains a large model then uses it as a teacher to train a more compact one aimed at approximating or mimicking the function learned by the large model.

The second factor is arithmetic operations in which the most intensive are multiplications. Compared to additions, they are three time more expensive in 32-bit floating-point, and above 30 time more expensive in 32-bit integer [Horowitz, 2014]. This factor becomes acute when considering large models. Arithmetic approximation proposes ways to tackle intensive multiplications [Cong and Xiao, 2014, Lavi et al., 2020, Chen et al., 2020a]. For instance, several solutions exploit the computation structure of deep layers to reduce the number of multiplications, most notably Fast Fourier Transform, Winograd’s algorithm

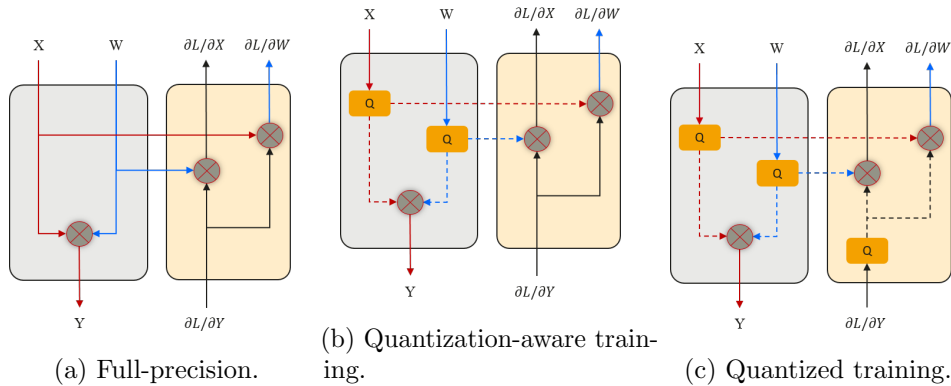


Figure 3: Data precision modalities during inference and training.

transforms, and Strassen’s algorithm-based approach [Sze et al., 2020a].

Data bitwidth is the third factor that affects computational efficiency. Typically, all weights and signals are considered to be real numbers represented by 32-bit floating-point format. Quantization reduces the memory usage by reducing this number of bits to represent each parameter and activation, for instance to a 16-bit, or even 8-bit format, with acceptable degradation of the prediction accuracy. It has been observed [Gholami et al., 2022] that quantization appears to be among the most efficient approaches regarding lower efforts and consistent gains it can achieve as compared to the other ones. Quantization methods can be classified into post-training quantization (i.e., quantized inference) [Fei et al., 2022] that quantizes a full-precision trained model, quantization-aware training [Gupta et al., 2015, Zhang et al., 2018, Jin et al., 2021, Yamamoto, 2021, Huang et al., 2021, Umuroglu et al., 2017], and quantized training [Chen et al., 2020b, Sun et al., 2020, Yang et al., 2022b, Chmiel et al., 2021]. Compared to the continuous operation, cf. Fig. 3a, quantization-aware training, cf. Fig. 3b, only quantizes the forward dataflows while keeping the training specific ones at full-precision. When the quantization function is the sign function, the resulting method becomes network binarization as described in the introduction. Quantized training in addition quantizes the backpropagated gradient. It however still keeps the weight gradient in full-precision for gradient descent optimizer, cf. Fig. 3c.

The above approaches have been mainly driven by the cost of arithmetic operations, i.e., aimed at reducing the number of floating-point operations (FLOPS) or per-operation cost. Even in the quantization approaches, although lowering data bitwidth is beneficial to both computation and data movement cost reduction (at the expense of performance loss), the design attention has been mainly attached to its effect on the computation. It has been revealed that the number of operations does not directly map to the actual computing hardware [Sze et al., 2017, 2020b, Rutter, 2001, Yang et al., 2017a, Strubell et al., 2019]. Instead, the energy consumption is a prime measure of computing efficiency. Besides, memory footprint, latency, and silicon area are important factors of consideration. [García-Martín et al., 2019] advocates that a reason of this lack of consideration by the machine learning community is due to possible unfamiliarity with energy consumption estimation as well as the lack of power models in the existing deep learning platforms such as TensorFlow, PyTorch, and MindSpore. Actually, energy consumption is due to not only computation but also data movement, which is often the

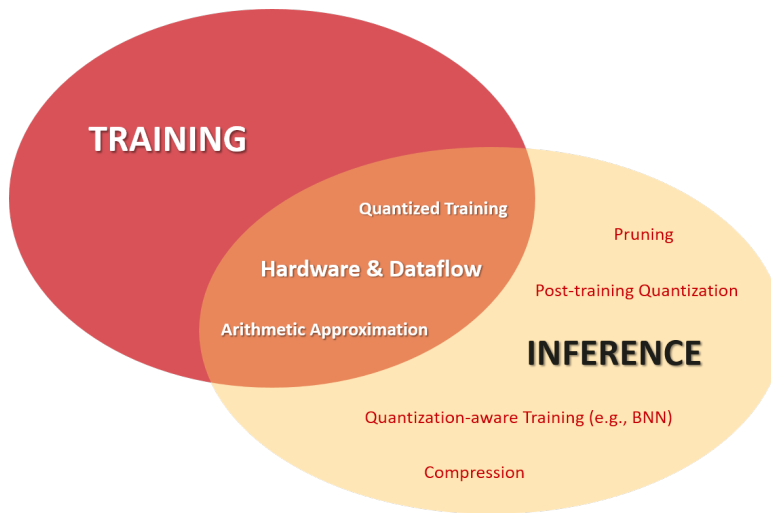


Figure 4: Overview of existing approaches and their benefits.

dominant part. It is strictly tied to the system specification and architecture, requiring specific knowledge of computing systems and making it very hard to estimate or predict at a high level of precision. It also means that system architecture, memory hierarchy, data throughput, and dataflow constitute the fourth factor of deep models' computational efficiency. On one hand, chip design has to trade off between the need of increasing near compute cache capacity, silicon area limitation, and energy consumption. In-memory or near-memory computing technologies [Grimm and Verma, 2022, Verma et al., 2019] have been proposed that consist in performing the compute inside or nearest to the memory [Sebastian et al., 2020, Alnatsheh et al., 2023], hence reducing the data movement cost. New hardware technologies [Yu and Chen, 2016, Yang et al., 2022a] have been also investigated that increase the data movement efficiency. On the other hand, due to excessive large dimensions of deep models, off-chip memory remains mandatory. This comes the von Neumann bottleneck [Zhang et al., 2022a] that refers to an exponential increase of the energy cost of moving data between off-chip memory and the compute unit. In consequence, dataflow design [Kwon et al., 2019] is a very important research area which aims at maximizing the data reuse so as to minimize the data movement cost. It is indeed a NP-hard problem [Yang et al., 2020] in particular for deep layers that exhibit high reuse patterns such as convolution layers. Stationary dataflows have been a prominent strategy that proposes keeping one or several dataflows stationary in or near the compute unit. Most practical designs are input stationary, output stationary, weight stationary, and row stationary [Chen et al., 2016].

Despite a lot of effort that has been given to deal with the computational intensiveness of deep models, except hardware and dataflow design that provides accelerated processing, most attention has been given to the inference complexity, for instance model compression, quantized inference, and quantization-aware training, cf. Fig. 4.

3 Design Insight and Method Introduction

Boolean neuron is considered as a Boolean function. Besides the well-known non-linearity requirement, are there any other properties that Boolean neuron function should satisfy for the network learning capability? Let us take an example using Reed-Muller codes (RMC) [MacWilliams and Sloane, 1977] as the neuron function. For instance, as the 2nd order RMC of size $m \geq 2$, the neuron is formulated as: $y = w_0 + \sum_{i=1}^m w_i x_i + \sum_{1 \leq i < j \leq m} w_{ij} x_i x_j$, where output y , weights (w_i) , $(w_{i,j})$, and inputs (x_i) are binary, and the sums are in the binary field, i.e., modulo 2. No additional activation function is used since this model is non-linear of the inputs, and the weights are trained by the decoding mechanism provided by this code. Unfortunately, networks built on this model do not generalize in our experiments. Analyzing the reason behind led to an intuition that the neuron function instead should be *elastic* in the sense that it should possess both responsive and absorptive regions in order to discriminate classes while being able to contract the points of the same class, which is not the case of this model. It implies that at some point inside the neuron’s input-output transformation, the neuron needs to be embedded in a richer domain such as integer or real.

Based on that understanding, the design proposed in the following is an effort to conciliate this intuition and the motivation of keeping the neuron in binary. Let (w_0, w_1, w_2, \dots) and (x_1, x_2, \dots) be Boolean numbers, and B be a Boolean logic operator such as AND, OR, XOR, XNOR which outputs 0 in place of False, and 1 in place of True. Define:

$$s = w_0 + \sum_i B(w_i, x_i), \quad (1)$$

where the sums are in the integer domain, which can be implemented in circuit using POPCOUNT. Let τ be a scalar, define:

$$y = \begin{cases} \text{T}, & \text{if } s \geq \tau \\ \text{F}, & \text{if } s < \tau \end{cases}. \quad (2)$$

This describes the neuron that we want to have for which (w_i) and (x_i) are Boolean weights and Boolean inputs, τ is threshold, and s is the pre-activation. This is indeed a restricted case of the McCulloch–Pitts neuron in which the weights are now constrained to Boolean numbers. Specifically, it also takes advantage of the Logic Threshold Gate (LTG) proposed by [McCulloch and Pitts, 1943] which includes both summation and decision such that “the decision can be made within the gate itself so that a pure binary output is produced” [Hampel and Winder, 1971], hence no need of storing the integer pre-activation s during the inference. LTG today has hardware implementation in standard CMOS logic [Maan et al., 2017]. On the other hand, the step activation function used in (2) contains one responsive point and two absorptive regions at the two sides of the threshold. This model therefore satisfies our initial design target. Historically, McCulloch–Pitts neuron has been enriched until the use of differentiable activation function and continuous variables which allow the direct employment of the gradient descent training, leading to both the success and computational intensiveness of today’s deep learning. Instead, we restrict it towards fully Boolean and propose in the following a method to train deep models of this Boolean neuron directly in the Boolean domain.

Instead of confronting a combinatorial problem of Boolean network training, we ask the question differently: as each weight only admits two values, should we keep or invert

its current value? If we can construct a rule for making such a decision, the problem can be solved. Let us take a toy example. Consider a XOR neuron, i.e., $\mathbf{B} = \mathbf{xor}$. If we are given a signal z that is back-propagated from the down-stream and indicates how the conditional/residual loss function at this stage varies with the neuron’s forward output, then the rule can be constructed as follows. Suppose that the received signal z indicates that the residual loss function increases with s . For weight w_i , we check its current value $\mathbf{xor}(w_i, x_i)$. If $\mathbf{xor}(w_i, x_i)$ is currently 1, it suffices to invert w_i so that the new weight w_i results in $\mathbf{xor}(w_i, x_i) = 0$ and makes s decreased. Hence, the first part of the method is that:

Q1) If given the backpropagation signal that expresses how the residual loss function varies w.r.t. the neuron’s forward output, *which weights to invert?*

To solve the above question, backpropagation signal z needs to be given. In the case that neuron’s downstream components provide the usual loss derivative, then z is given and completely expresses the expected information. In the other case where neuron’s downstream components do not have loss derivative, the second question to be solved is:

Q2) *What is the backpropagation signal of Boolean neurons?*

4 Boolean Variation

4.1 Preliminary

Let \mathbf{B} denote the set $\{\mathbf{T}, \mathbf{F}\}$ equipped with Boolean logic.

Definition 4.1. *Order relations ‘<’ and ‘>’ in \mathbf{B} are defined as follows:*

$$\mathbf{F} < \mathbf{T}, \quad \mathbf{T} > \mathbf{F}. \quad (3)$$

Definition 4.2. *For $x, y \in \mathbf{B}$, define:*

$$\delta(x \rightarrow y) \stackrel{\text{def}}{=} \begin{cases} \mathbf{T}, & \text{if } y > x, \\ 0, & \text{if } y = x, \\ \mathbf{F}, & \text{if } y < x, \end{cases} \quad (4)$$

which is called the variation of x to y .

Definition 4.3 (Three-valued logic). *Define $\mathbf{M} = \mathbf{B} \cup \{0\}$ with logic connectives specified in Tab. 1.*

\mathbf{M} is an extension of the Boolean logic by adding element 0 whose meaning is “ignored”, and the connection of its logic connectives to those of Boolean logic can be expressed as follows. Let l be a logic connective, denote by $l_{\mathbf{M}}$ and $l_{\mathbf{B}}$ when it is applied in \mathbf{M} and in \mathbf{B} , respectively. Then, what defined Definition 4.3 can be expressed as follows:

$$l_{\mathbf{M}}(a, b) = \begin{cases} 0, & \text{if } a = 0 \text{ or } b = 0, \\ l_{\mathbf{B}}(a, b), & \text{otherwise.} \end{cases} \quad (5)$$

In the sequel, the following notations are used:

a	$\neg a$
T	F
0	0
F	T

(a) Negation

and		b		
		T	0	F
a	T	T	0	F
	0	0	0	0
	F	F	0	F

(b) AND

or		b		
		T	0	F
a	T	T	0	T
	0	0	0	0
	F	T	0	F

(c) OR

xor		b		
		T	0	F
a	T	F	0	T
	0	0	0	0
	F	T	0	F

(d) XOR

xnor		b		
		T	0	F
a	T	T	0	F
	0	0	0	0
	F	F	0	T

(e) XNOR

Table 1: Logic connectives of the three-value logic \mathbf{M} .

- \mathbf{R} : the real set; \mathbf{D} : a discrete set; \mathbf{N} : a numeric set, e.g., \mathbf{R} or \mathbf{D} ;
- \mathbf{L} : a logic set, e.g., \mathbf{B} or \mathbf{M} .
- \mathbf{S} : a certain domain that can be any of \mathbf{L} or \mathbf{N} .

Definition 4.4. *The magnitude of a variable x , denoted $|x|$, is defined as follows:*

- $x \in \mathbf{B}$: $|x| = 1$.
- $x \in \mathbf{M}$: $|x| = 0$ if $x = 0$, and $|x| = 1$ otherwise.
- $x \in \mathbf{N}$: $|x|$ is defined as its usual absolute value.

Definition 4.5 (Type conversion). *Define:*

$$\begin{aligned}
 & p: \mathbf{N} \rightarrow \mathbf{L} \\
 & x \mapsto x_L = p(x) = \begin{cases} \text{T,} & \text{if } x > 0, \\ 0, & \text{if } x = 0, \\ \text{F,} & \text{if } x < 0. \end{cases} \quad (6)
 \end{aligned}$$

$$\begin{aligned}
 & e: \mathbf{L} \rightarrow \mathbf{N} \\
 & a \mapsto a_N = e(a) = \begin{cases} +1, & \text{if } a = \text{T,} \\ 0, & \text{if } a = 0, \\ -1, & \text{if } a = \text{F.} \end{cases} \quad (7)
 \end{aligned}$$

p projects a numeric type in logic, and e embeds a logic type in numeric. It is clear that for $x, y \in \mathbf{N}$:

$$x = y \Leftrightarrow |x| = |y| \text{ and } p(x) = p(y). \quad (8)$$

Definition 4.6 (Mixed-type logic). *For l a logic connective of \mathbf{L} and two variables a, b , operation $c = l(a, b)$ is defined such that $|c| = |a||b|$ and $c_L = l(a_L, b_L)$.*

Proposition 4.7. *The following properties hold:*

1. $a \in \mathbf{L}, x \in \mathbf{N}$:

$$\mathbf{xnor}(a, x) = \begin{cases} x, & \text{if } a = \mathbf{T}, \\ 0, & \text{if } a = 0, \\ -x, & \text{if } a = \mathbf{F}. \end{cases} \quad (9)$$

2. $x, y \in \mathbf{N}$: $\mathbf{xnor}(x, y) = xy$.

3. $x \in \{\mathbf{L}, \mathbf{N}\}, y, z \in \mathbf{N}$: $\mathbf{xnor}(x, y + z) = \mathbf{xnor}(x, y) + \mathbf{xnor}(x, z)$.

4. $x \in \{\mathbf{L}, \mathbf{N}\}, y, \lambda \in \mathbf{N}$: $\mathbf{xnor}(x, \lambda y) = \lambda \mathbf{xnor}(x, y)$.

5. $x \in \{\mathbf{L}, \mathbf{N}\}, y \in \mathbf{N}$: $\mathbf{xnor}(x, y) = -\mathbf{xnor}(x, y)$.

Proof. The proof follows definitions 4.6 and 4.5.

- Following Definition 4.3 we have $\forall t \in \mathbf{M}, \mathbf{xnor}(\mathbf{T}, t) = t, \mathbf{xnor}(\mathbf{F}, t) = \neg t$, and $\mathbf{xnor}(0, t) = 0$. Put $v = \mathbf{xnor}(a, x)$. We have $|v| = |x|$ and $v_L = \mathbf{xnor}(a, x_L)$. Hence, $a = 0 \Rightarrow v_L = 0 \Rightarrow v = 0$; $a = \mathbf{T} \Rightarrow v_L = x_L \Rightarrow v = x$; $a = \mathbf{F} \Rightarrow v_L = \neg x_L \Rightarrow v = -x$. Hence (1).
- The result is trivial if $x = 0$ or $y = 0$. For $x, y \neq 0$, put $v = \mathbf{xnor}(x, y)$, we have $|v| = |x||y|$ and $v_L = \mathbf{xnor}(x_L, y_L)$. According to Definition 4.5, if $\text{sign}(x) = \text{sign}(y)$, we have $v_L = \mathbf{T} \Rightarrow v = |x||y| = xy$. Otherwise, i.e., $\text{sign}(x) = -\text{sign}(y)$, $v_L = \mathbf{F} \Rightarrow v = -|x||y| = xy$. Hence (2).
- (3) and (4) follow (1) for $x \in \mathbf{L}$ and follow (2) for $x \in \mathbf{N}$.
- For (5), write $u = \mathbf{xnor}(x, y)$ and $v = \mathbf{xnor}(x, y)$, we have $|u| = |v|$ and $u_L = \mathbf{xnor}(x_L, y_L) = \neg \mathbf{xnor}(x_L, y_L) = \neg v_L$. Thus, $\text{sign}(u) = -\text{sign}(v) \Rightarrow u = -v$. \square

4.2 Variation Calculus

Definition 4.8. For $f \in \mathcal{F}(\mathbf{B}, \mathbf{B})$, the variation of f w.r.t. its variable, denoted f' , is defined as follows:

$$\begin{aligned} f' : \mathbf{B} &\rightarrow \mathbf{M} \\ x &\mapsto \mathbf{xnor}(\delta(x \rightarrow \neg x), \delta f(x \rightarrow \neg x)). \end{aligned}$$

Intuitively, the variation of f is True if f varies in the same direction with x .

Notation 1. We use notation $\delta f(x)/\delta x$ to denote the variation of a function f w.r.t. a variable x , i.e.,

$$\frac{\delta f(x)}{\delta x} := f'(x). \quad (10)$$

Example 1. For $f = \mathbf{xnor}(a, b)$ with $a, b \in \mathbf{B}$, the variation of f w.r.t. each variable according to Definition 4.8 can be derived by establishing a truth table as in Tab. 2 from which we obtain:

$$f'_a(b) = \neg a. \quad (11)$$

Proposition 4.9. For $f, g \in \mathcal{F}(\mathbf{B}, \mathbf{B})$, $\forall x, y \in \mathbf{B}$ the following properties hold:

a	b	$\neg b$	$\delta(b \rightarrow \neg b)$	$f(a, b)$	$f(a, \neg b)$	$\delta f_a(b \rightarrow \neg b)$	$f'_a(b)$
T	T	F	F	F	T	T	F
T	F	T	T	T	F	F	F
F	T	F	F	T	F	F	T
F	F	T	T	F	T	T	T

Table 2: Variation truth table of **xnor**.

1. $\delta f(x \rightarrow y) = \mathbf{xnor}(\delta(x \rightarrow y), f'(x))$.
2. $(\neg f)'(x) = \neg f'(x)$.
3. $(g \circ f)'(x) = \mathbf{xnor}(g'(f(x)), f'(x))$.

Proof. The proof is by definition:

1. $\forall x, y \in \mathbf{B}$, there are two cases. If $y = x$, then the result is trivial. Otherwise, i.e., $y = \neg x$, by definition we have:

$$\begin{aligned} f'(x) &= \mathbf{xnor}(\delta(x \rightarrow \neg x), \delta f(x \rightarrow \neg x)) \\ \Leftrightarrow \delta f(x \rightarrow \neg x) &= \mathbf{xnor}(\delta(x \rightarrow \neg x), f'(x)). \end{aligned}$$

Hence the result.

2. $\forall x, y \in \mathbf{B}$, it is easy to verify by truth table that $\delta(\neg f(x \rightarrow y)) = \neg \delta f(x \rightarrow y)$. Hence, by definition,

$$\begin{aligned} (\neg f)'(x) &= \mathbf{xnor}(\delta(x \rightarrow \neg x), \delta(\neg f(x \rightarrow \neg x))) \\ &= \mathbf{xnor}(\delta(x \rightarrow \neg x), \neg \delta f(x \rightarrow \neg x)) \\ &= \neg \mathbf{xnor}(\delta(x \rightarrow \neg x), \delta f(x \rightarrow \neg x)) \\ &= \neg f'(x). \end{aligned}$$

3. Using definition, property (i), and associativity of **xnor**, $\forall x \in \mathbf{B}$ we have:

$$\begin{aligned} (g \circ f)'(x) &= \mathbf{xnor}(\delta(x \rightarrow \neg x), \delta g(f(x) \rightarrow f(\neg x))) \\ &= \mathbf{xnor}(\delta(x \rightarrow \neg x), \mathbf{xnor}(\delta f(x \rightarrow \neg x), g'(f(x)))) \\ &= \mathbf{xnor}(g'(f(x)), \mathbf{xnor}(\delta(x \rightarrow \neg x), \delta f(x \rightarrow \neg x))) \\ &= \mathbf{xnor}(g'(f(x)), f'(x)). \end{aligned}$$

□

Definition 4.10. For $f \in \mathcal{F}(\mathbf{B}, \mathbf{N})$, the variation of f w.r.t. its variable, denoted f' , is defined as follows:

$$\begin{aligned} f' : \mathbf{B} &\rightarrow \mathbf{N} \\ x &\mapsto \mathbf{xnor}(\delta(x \rightarrow \neg x), \delta f(x \rightarrow \neg x)). \end{aligned}$$

Proposition 4.11. For $f \in \mathcal{F}(\mathbf{B}, \mathbf{N})$, the following properties hold:

1. $x, y \in \mathbf{B}$: $\delta f(x \rightarrow y) = \mathbf{xnor}(\delta(x \rightarrow y), f'(x))$.
2. $x \in \mathbf{B}, \alpha \in \mathbf{N}$: $(\alpha f)'(x) = \alpha f'(x)$.
3. $x \in \mathbf{B}, g \in \mathcal{F}(\mathbf{B}, \mathbf{N})$: $(f + g)'(x) = f'(x) + g'(x)$.

Proof. The proof is as follows:

1. For $x, y \in \mathbf{B}$. Firstly, the result is trivial if $y = x$. For $y \neq x$, i.e., $y = \neg x$, by definition:

$$f'(x) = \mathbf{xnor}(\delta(x \rightarrow \neg x), \delta f(x \rightarrow \neg x)).$$

Hence, $|\delta f(x \rightarrow \neg x)| = |f'(x)|$ since $|\delta(x \rightarrow \neg x)| = 1$, and

$$\begin{aligned} p(f'(x)) &= \mathbf{xnor}(\delta(x \rightarrow \neg x), p(\delta f(x \rightarrow \neg x))) \\ \Leftrightarrow p(\delta f(x \rightarrow \neg x)) &= \mathbf{xnor}(\delta(x \rightarrow \neg x), p(f'(x))), \end{aligned}$$

where p is the logic projector (6). Thus, $f(x \rightarrow \neg x) = \mathbf{xnor}(\delta(x \rightarrow \neg x), f'(x))$. Hence the result.

2. Firstly $\forall x, y \in \mathbf{B}$, we have

$$\delta(\alpha f(x \rightarrow y)) = \alpha f(y) - \alpha f(x) = \alpha \delta f(x \rightarrow y).$$

Hence, by definition,

$$\begin{aligned} (\alpha f)'(x) &= \mathbf{xnor}(\delta(x \rightarrow \neg x), \delta(\alpha f(x \rightarrow \neg x))) \\ &= \mathbf{xnor}(\delta(x \rightarrow \neg x), \alpha \delta f(x \rightarrow \neg x)) \\ &= \alpha \mathbf{xnor}(\delta(x \rightarrow \neg x), \delta f(x \rightarrow \neg x)), \text{ due to Proposition 4.7(4)} \\ &= \alpha f'(x). \end{aligned}$$

3. For $f, g \in \mathcal{F}(\mathbf{B}, \mathbf{N})$,

$$\begin{aligned} (f + g)'(x) &= \mathbf{xnor}(\delta(x \rightarrow \neg x), \delta(f + g)(x \rightarrow \neg x)) \\ &= \mathbf{xnor}(\delta(x \rightarrow \neg x), \delta f(x \rightarrow \neg x) + \delta g(x \rightarrow \neg x)) \\ &\stackrel{(*)}{=} \mathbf{xnor}(\delta(x \rightarrow \neg x), \delta f(x \rightarrow \neg x)) + \mathbf{xnor}(\delta(x \rightarrow \neg x), \delta g(x \rightarrow \neg x)), \\ &= f'(x) + g'(x), \end{aligned}$$

where (*) is due to Proposition 4.7(3). □

For discrete-variable functions, recall that the discrete derivative of $f \in \mathcal{F}(\mathbf{D}, \mathbf{N})$ has been defined in the literature as $f'(n) = f(n + 1) - f(n)$. With the logic variation as previously introduced in this section, we can have a more generic definition of the variation of a discrete-variable function as follows.

Definition 4.12. For $f \in \mathcal{F}(\mathbf{D}, \mathbf{S})$, the variation of f w.r.t. its variable is defined as follows:

$$\begin{aligned} f' : \mathbf{D} &\rightarrow \mathbf{S} \\ x &\mapsto \delta f(x \rightarrow x + 1), \end{aligned}$$

where δf is in the sense of the variation defined in \mathbf{S} .

Proposition 4.13 (Composition rules). *The following properties hold:*

1. For $\mathbf{B} \xrightarrow{f} \mathbf{B} \xrightarrow{g} \mathbf{S}$: $(g \circ f)'(x) = \mathbf{xnor}(g'(f(x)), f'(x))$, $\forall x \in \mathbf{B}$.
2. For $\mathbf{B} \xrightarrow{f} \mathbf{D} \xrightarrow{g} \mathbf{S}$, $x \in \mathbf{B}$, if $|f'(x)| \leq 1$ and $g'(f(x)) = g'(f(x) - 1)$, then:

$$(g \circ f)'(x) = \mathbf{xnor}(g'(f(x)), f'(x)).$$

Proof. The proof is as follows.

1. The case of $\mathbf{B} \xrightarrow{f} \mathbf{B} \xrightarrow{g} \mathbf{B}$ is obtained from Proposition 4.9(3). For $\mathbf{B} \xrightarrow{f} \mathbf{B} \xrightarrow{g} \mathbf{N}$, by using Proposition 4.11(1), the proof is similar to that of Proposition 4.9(3).
2. By definition, we have

$$(g \circ f)'(x) = \mathbf{xnor}(\delta(x \rightarrow \neg x), \delta g(f(x) \rightarrow f(\neg x))). \quad (12)$$

Using property (1) of Proposition 4.11, we have:

$$\begin{aligned} f(\neg x) &= f(x) + \delta f(x \rightarrow \neg x) \\ &= f(x) + \mathbf{xnor}(\delta(x \rightarrow \neg x), f'(x)). \end{aligned} \quad (13)$$

Applying (13) back to (12), the result is trivial if $f'(x) = 0$. The remaining case is $|f'(x)| = 1$ for which we have $\mathbf{xnor}(\delta(x \rightarrow \neg x), f'(x)) = \pm 1$. First, for $\mathbf{xnor}(\delta(x \rightarrow \neg x), f'(x)) = 1$, we have:

$$\begin{aligned} \delta g(f(x) \rightarrow f(\neg x)) &= \delta g(f(x) \rightarrow f(x) + 1) \\ &= g'(f(x)) \\ &= \mathbf{xnor}(g'(f(x)), 1) \\ &= \mathbf{xnor}(g'(f(x)), \mathbf{xnor}(\delta(x \rightarrow \neg x), f'(x))). \end{aligned} \quad (14)$$

Substitute (14) back to (12), we obtain:

$$\begin{aligned} (g \circ f)'(x) &= \mathbf{xnor}(\delta(x \rightarrow \neg x), \delta g(f(x) \rightarrow f(\neg x))) \\ &= \mathbf{xnor}(\delta(x \rightarrow \neg x), \mathbf{xnor}(g'(f(x)), \mathbf{xnor}(\delta(x \rightarrow \neg x), f'(x)))) \\ &= \mathbf{xnor}(g'(f(x)), f'(x)), \end{aligned}$$

where that last equality is by the associativity of \mathbf{xnor} and that $\mathbf{xnor}(x, x) = \mathbf{T}$ for $x \in \mathbf{B}$. Similarly, for $\mathbf{xnor}(\delta(x \rightarrow \neg x), f'(x)) = -1$, we have:

$$\begin{aligned} \delta g(f(x) \rightarrow f(\neg x)) &= \delta g(f(x) \rightarrow f(x) - 1) \\ &= -g'(f(x) - 1) \\ &= \mathbf{xnor}(g'(f(x) - 1), -1) \\ &= \mathbf{xnor}(g'(f(x) - 1), \mathbf{xnor}(\delta(x \rightarrow \neg x), f'(x))). \end{aligned} \quad (15)$$

Substitute (15) back to (12) and use the assumption that $g'(f(x)) = g'(f(x) - 1)$, we have:

$$\begin{aligned} (g \circ f)'(x) &= \mathbf{xnor}(\delta(x \rightarrow \neg x), \delta g(f(x) \rightarrow f(\neg x))) \\ &= \mathbf{xnor}(\delta(x \rightarrow \neg x), \mathbf{xnor}(g'(f(x) - 1), \mathbf{xnor}(\delta(x \rightarrow \neg x), f'(x)))) \\ &= \mathbf{xnor}(g'(f(x)), f'(x)). \end{aligned}$$

Hence the result. □

The above formulation is extended to the multivariate case in a straightforward manner. In the following, we show one example with Boolean functions.

Definition 4.14. For $\mathbf{x} = (x_1, \dots, x_n) \in \mathbf{B}^n$, $n \geq 1$, and $1 \leq i \leq n$, denote:

$$\mathbf{x}_{-i} := (x_1, \dots, x_{i-1}, \neg x_i, x_{i+1}, \dots, x_n).$$

For $f \in \mathcal{F}(\mathbf{B}^n, \mathbf{B})$, the (partial) variation of f w.r.t. x_i , denoted $f'_i(\mathbf{x})$ and $\frac{\delta f(\mathbf{x})}{\delta x_i}$, is defined as follows:

$$f'_i(\mathbf{x}) = \frac{\delta f(\mathbf{x})}{\delta x_i} \stackrel{\text{def}}{=} \mathbf{xnor}(\delta(x_i \rightarrow \neg x_i), \delta f(\mathbf{x} \rightarrow \mathbf{x}_{-i})). \quad (16)$$

It is easy to show that f'_i has the same properties as in Proposition 4.9. For instance, the composition is as follows.

Proposition 4.15. For $f \in \mathcal{F}(\mathbf{B}^n, \mathbf{B})$, $g \in \mathcal{F}(\mathbf{B}, \mathbf{B})$, $1 \leq i \leq n$, we have:

$$(g \circ f)'_i(\mathbf{x}) = \mathbf{xnor}(g'(f(\mathbf{x})), f'_i(\mathbf{x})). \quad (17)$$

Proof. By definition:

$$\begin{aligned} (g \circ f)'_i(\mathbf{x}) &= \mathbf{xnor}(\delta(x_i \rightarrow \neg x_i), \delta g(f(\mathbf{x}) \rightarrow f(\mathbf{x}_{-i}))) \\ &= \mathbf{xnor}(\delta(x_i \rightarrow \neg x_i), \mathbf{xnor}(\delta f(\mathbf{x} \rightarrow \mathbf{x}_{-i}), g'(f(\mathbf{x})))) , \text{ Proposition 4.9(1)} \\ &= \mathbf{xnor}(\mathbf{xnor}(\delta(x_i \rightarrow \neg x_i), \delta f(\mathbf{x} \rightarrow \mathbf{x}_{-i})), g'(f(\mathbf{x}))) \\ &= \mathbf{xnor}(g'(f(\mathbf{x})), f'_i(\mathbf{x})). \quad \square \end{aligned}$$

5 Boolean Logic BackPropagation

With the notions introduced in Section 4, we can write signals involved in the backpropagation process as shown in Fig. 5. Therein, layer l is a Boolean layer of consideration. For the sake of presentation simplicity, layer l is assumed a fully connected layer, and:

$$x_{k,j}^{l+1} = w_{0,j}^l + \sum_{i=1}^m \mathbf{B}(x_{k,i}^l, w_{i,j}^l), \quad 1 \leq j \leq n, \quad (18)$$

where \mathbf{B} is the utilized Boolean logic, k denotes sample index in the batch, m and n are the usual layer input and output sizes. Layer l is connected to layer $l+1$ that can be an activation layer, a batch normalization, an arithmetic layer, or any others. Nature of $\delta L / \delta x_{k,j}^{l+1}$ depends on the property of layer $l+1$. For instance, it can be a usual gradient if layer $l+1$ is a real-valued arithmetic layer, or a Boolean variation if layer $l+1$ is a Boolean layer. Given $\delta L / \delta x_{k,j}^{l+1}$, Boolean layer l needs to optimize its Boolean weights and compute signal $\delta L / \delta x_{k,i}^l$ for the upstream.

5.1 Optimization Logic

With reference to Fig. 5, we develop logic for optimizing each weight $w_{i,j}^l$ of Boolean layer l . Following the intuition as previously described, we need to compute the variation

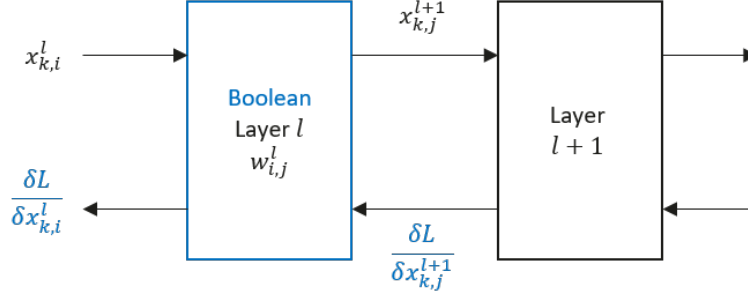


Figure 5: Illustration of signals with a Boolean linear layer. L denotes the loss function.

of the loss w.r.t. weight $w_{i,j}^l$, i.e., $\delta L / \delta w_{i,j}^l$. Using Proposition ??, for data sample k in the batch, we can have:

$$q_{i,j,k}^l := \frac{\delta L}{\delta w_{i,j}^l} \Big|_k = \mathbf{xnor} \left(\frac{\delta L}{\delta x_{k,j}^{l+1}}, \frac{\delta x_{k,j}^{l+1}}{\delta w_{i,j}^l} \right), \quad (19)$$

for which we need to derive $\delta x_{k,j}^{l+1} / \delta w_{i,j}^l$ taking into account the utilized logic B. With reference to (18), the variation of $x_{k,j}^{l+1}$ w.r.t., $w_{i,j}^l$ as defined in Section 4 can be obtained by simply establishing its truth table. For XOR neuron, its variation truth table is given in Tab. 3 from which we can obtain:

$$\text{XOR neuron: } \frac{\delta x_{k,j}^{l+1}}{\delta w_{i,j}^l} = \neg x_{k,i}^l. \quad (20)$$

Following the same method, one can obtain the result for any other Boolean logic. In particular, for XNOR neuron, given that $\mathbf{xnor} = \neg \mathbf{xor}$, we can directly obtain the following:

$$\text{XNOR neuron: } \frac{\delta x_{k,j}^{l+1}}{\delta w_{i,j}^l} = x_{k,i}^l. \quad (21)$$

Hence, per-sample variation $q_{i,j,k}^l$ of weight $w_{i,j}^l$ can be obtained for any utilized logic B.

We now aggregate it over the batch dimension. Due to (19), datatype of $\delta L / \delta x_{k,j}^{l+1}$ decides the that of $q_{i,j,k}^l$, i.e., Boolean or not. In the case that $\delta L / \delta x_{k,j}^{l+1}$ is non Boolean, so is $q_{i,j,k}^l$, and the aggregation is performed by real summation. In the case that $q_{i,j,k}^l$ is Boolean, the aggregation can be based on majority rule, i.e., the difference between the number of True and of False. Both cases can be formulated as follows.

Definition 5.1. Let $\mathbf{1}(\cdot)$ be the indicator function. For $b \in \mathbf{B}$ and variable x , define:

$$\mathbf{1}(x = b) = \begin{cases} 1, & \text{if } x_{\text{bool}} = b, \\ 0, & \text{otherwise.} \end{cases} \quad (22)$$

The aggregation of weight variation is given as:

$$q_{i,j}^l := \frac{\delta L}{\delta w_{i,j}^l} = \sum_k \mathbf{1}(q_{i,j,k}^l = \text{T}) |q_{i,j,k}^l| - \sum_k \mathbf{1}(q_{i,j,k}^l = \text{F}) |q_{i,j,k}^l|. \quad (23)$$

Table 3: Variation truth table of XOR neuron.

$x_{k,i}^l$	$w_{i,j}^l$	$\neg w_{i,j}^l$	$\delta w_{i,j}^l$	$\delta x_{k,j}^{l+1}$	$\delta x_{k,j}^{l+1} / \delta w_{i,j}^l$
T	T	F	F	T	F
T	F	T	T	F	F
F	T	F	F	F	T
F	F	T	T	T	T

Table 4: Optimization logic truth table.

$\delta L / \delta w_{i,j}^l$	$w_{i,j}^l$	Action
T	T	Invert
T	F	Keep
F	T	Keep
F	F	Invert

Given this information, the rule for inverting $w_{i,j}^l$ subjected to decreasing the loss is simply given according to its definition as:

$$\boxed{w_{i,j}^l = \neg w_{i,j}^l \text{ if } \mathbf{xnor}(q_{i,j}^l, w_{i,j}^l) = \text{T}.} \quad (24)$$

It can be also simply given by truth table Tab. 4. Equation 24 is the core optimization logic based on which more sophisticated forms of optimizer can be developed in the same manner as different methods such as Adam have been developed from the basic gradient descent principle. For instance, the following is one optimizer that accumulates $q_{i,j}^l$ over training iterations. Denote by $q_{i,j}^{l,t}$ the optimization signal at iteration t , and by $m_{i,j}^{l,t}$ its accumulator with $m_{i,j}^{l,0} := 0$ and:

$$m_{i,j}^{l,t+1} = \beta^t m_{i,j}^{l,t} + \eta^t q_{i,j}^{l,t+1}, \quad (25)$$

where η^t is an accumulation factor that can be tuned as a hyper-parameter, and β^t is an auto-regularizing factor that expresses the system’s state at time t . Its usage is linked to brain plasticity [Fuchs et al., 2014] and Hebbian theory [Hebb, 2005], stating that “cells that fire together wire together”, forcing weights to adapt to their neighborhood during the learning process. For the chosen weight’s neighborhood, for instance, neuron, layer, or network level, β^t is given as:

$$\beta^t = \frac{\text{Nb of unchanged weights at } t}{\text{Total number of weights}}. \quad (26)$$

In the experiments presented later, β^t is set to per-layer basis and initialized as $\beta^0 = 1$. Finally, the accumulation-based optimizer is described in Appendix 1.

Algorithm 1: Accumulate optimizer

Input : η^0 –accumulation rate, T –number of iterations;

```
1 Init
2   |  $\beta^0 = 1$ ;
3   |  $m_{i,j}^{l,0} = 0$ ;
4 end
5 for  $t = 0, \dots, T - 1$  do
6   | Compute  $q_{i,j}^{l,t+1}$  ;
7   | Update  $m_{i,j}^{l,t+1}$  ;
8   | if  $\mathbf{xnor}(m_{i,j}^{l,t+1}, w_{i,j}^{l,t}) = \text{T}$  then
9     |    $w_{i,j}^{l,t+1} \leftarrow \neg w_{i,j}^{l,t}$ ;
10    |    $m_{i,j}^{l,t+1} \leftarrow 0$ ;
11  | else
12    |    $w_{i,j}^{l,t+1} \leftarrow w_{i,j}^{l,t}$ ;
13  | end
14  | Update  $\eta^{t+1}$ ;
15  | Update  $\beta^{t+1}$ ;
16 end
```

5.2 Backpropagation Logic

In this section, we compute the backpropagation signal $\delta L / \delta x_{k,i}^l$ of the Boolean layer l . Following Proposition ??, for each received signal $\delta L / \delta x_{k,j}^{l+1}$, we have:

$$g_{k,i,j}^l := \frac{\delta L}{\delta x_{k,i}^l} \Big|_j = \mathbf{xnor} \left(\frac{\delta L}{\delta x_{k,j}^{l+1}}, \frac{\delta x_{k,j}^{l+1}}{\delta x_{k,i}^l} \right), \quad (27)$$

for which $\delta x_{k,j}^{l+1} / \delta x_{k,i}^l$ needs to be derived taking into account the utilized logic B as in Section 5.1. In particular, using the symmetry of Boolean logic, we can directly obtain it for XOR neuron using (20), and for XNOR neuron using (21) as follows:

$$\frac{\delta x_{k,j}^{l+1}}{\delta x_{k,i}^l} = \begin{cases} \neg w_{i,j}^l, & \text{for XOR neuron,} \\ w_{i,j}^l, & \text{for XNOR neuron.} \end{cases} \quad (28)$$

Aggregating $g_{k,i,j}^l$ over the output dimension follows the same majority rule as described in Section 5.1. Hence,

$$\boxed{\frac{\delta L}{\delta x_{k,i}^l} = \sum_j \mathbf{1}(g_{k,i,j}^l = \text{T}) |g_{k,i,j}^l| - \sum_j \mathbf{1}(g_{k,i,j}^l = \text{F}) |g_{k,i,j}^l|.} \quad (29)$$

5.3 Preliminary Assessment

Tab. 5 shows a case study of this concept on CIFAR-10 with VGG-Small architecture. Therein, Boolean method is tested with 2 architectures: one without using batch

normalization, and the other using batch normalization and the activation from Liu et al. [2019].

Table 5: Experimental results on CIFAR-10 with VGG-Small.

Method	W/A	Training	Test Accu (%)
VGG-Small (FP) Zhang et al. [2018]	32/32	Latent	93.80
BinaryConnect Courbariaux et al. [2015]	1/32	Latent	90.10
XNOR-Net Rastegari et al. [2016]	1/1	Latent	89.83
BNN Hubara et al. [2017]	1/1	Latent	89.85
Boolean Logic w/o BN (Ours)	1/1	Boolean	90.29
Boolean Logic + BN (Ours)	1/1	Boolean	92.37

6 Conclusion

The notion of Boolean variation is introduced at the first time based on which Boolean logic backpropagation is proposed, replacing the gradient backpropagation. This is a new mathematical principle allowing for building and training deep models directly in Boolean domain with Boolean logic. Future investigations include evaluating performance and complexity gains in deep learning tasks, and applying it to different architectures including transformers.

References

- S. B. Akers, Jr. On a theory of Boolean functions. *Journal of the Society for Industrial and Applied Mathematics*, 7(4):487–498, 1959. doi: 10.1137/0107041. URL <https://doi.org/10.1137/0107041>.
- N. Alnatsheh, Y. Kim, J. Cho, and K. K. Choi. A novel 8T XNOR-SRAM: Computing-in-memory design for binary/ternary deep neural networks. *Electronics*, 12(4), 2023. ISSN 2079-9292. doi: 10.3390/electronics12040877. URL <https://www.mdpi.com/2079-9292/12/4/877>.
- C. Baldassi. Generalization learning in a perceptron with binary synapses. *J. Stat. Phys.*, 136(5):902–916, Sep 2009. ISSN 1572-9613. doi: 10.1007/s10955-009-9822-1. URL <https://doi.org/10.1007/s10955-009-9822-1>.
- C. Baldassi and A. Braunstein. A max-sum algorithm for training discrete neural networks. *J. Stat. Mech: Theory Exp.*, 2015(8):P08008, 2015.
- C. Baldassi, A. Ingrosso, C. Lucibello, L. Saglietti, and R. Zecchina. Subdominant dense clusters allow for simple learning and high computational performance in neural networks with discrete synapses. *Physical Review Letters*, 115(12):128101, 2015.
- J. Bethge, H. Yang, M. Bornstein, and C. Meinel. BinaryDenseNet: Developing an architecture for binary neural networks. In *Proceedings of the IEEE International Conference on Computer Vision Workshops*, pages 0–0, 2019.

- H. Chen, Y. Wang, C. Xu, B. Shi, C. Xu, Q. Tian, and C. Xu. AdderNet: Do we really need multiplications in deep learning? In *Proceedings of the IEEE/CVF Conference on Computer Vision and Pattern Recognition (CVPR)*, June 2020a.
- J. Chen, Y. Gai, Z. Yao, M. W. Mahoney, and J. E. Gonzalez. A statistical framework for low-bitwidth training of deep neural networks. In *Advances in Neural Information Processing Systems 33 (NeurIPS 2020)*, 2020b.
- Y.-H. Chen, T. Krishna, J. S. Emer, and V. Sze. Eyeriss: An energy-efficient reconfigurable accelerator for deep convolutional neural networks. *IEEE journal of solid-state circuits*, 52(1):127–138, 2016.
- Y. Cheng, D. Wang, P. Zhou, and T. Zhang. A survey of model compression and acceleration for deep neural networks. *arXiv preprint arXiv:1710.09282*, 2020.
- B. Chmiel, R. Banner, E. Hoffer, H. B. Yaacov, and D. Soudry. Logarithmic unbiased quantization: Simple 4-bit training in deep learning. *arXiv:2112.10769*, 2021. doi: 10.48550/ARXIV.2112.10769. URL <https://arxiv.org/abs/2112.10769>.
- J. Cong and B. Xiao. Minimizing computation in convolutional neural networks. In *Artificial Neural Networks and Machine Learning—ICANN 2014: 24th International Conference on Artificial Neural Networks, Hamburg, Germany, September 15-19, 2014. Proceedings 24*, pages 281–290. Springer, 2014.
- M. Courbariaux, Y. Bengio, and J.-P. David. BinaryConnect: Training deep neural networks with binary weights during propagations. In *Advances in Neural Information Processing Systems*, pages 3123–3131, 2015.
- W. Fei, W. Dai, C. Li, J. Zou, and H. Xiong. General bitwidth assignment for efficient deep convolutional neural network quantization. *IEEE Trans. Neural Netw. Learn. Syst.*, 33(10):5253–5267, 2022. doi: 10.1109/TNNLS.2021.3069886.
- E. Fuchs, G. Flügge, et al. Adult neuroplasticity: more than 40 years of research. *Neural plasticity*, 2014, 2014.
- E. García-Martín, C. F. Rodrigues, G. Riley, and H. Grahm. Estimation of energy consumption in machine learning. *J Parallel Distr Com*, 134:75–88, 2019.
- A. Gholami, S. Kim, Z. Dong, Z. Yao, M. W. Mahoney, and K. Keutzer. *Low-Power Computer Vision*, chapter A Survey of Quantization Methods for Efficient Neural Network Inference, pages 291–326. Chapman and Hall/CRC, 2022.
- C. Grimm and N. Verma. Neural network training on in-memory-computing hardware with radix-4 gradients. *IEEE Trans. Circuits Syst. I*, 69(10):4056–4068, 2022. doi: 10.1109/TCSI.2022.3185556.
- N. Guo, J. Bethge, C. Meinel, and H. Yang. Join the high accuracy club on ImageNet with a binary neural network ticket. *arXiv preprint arXiv:2211.12933*, 2022.
- S. Gupta, A. Agrawal, K. Gopalakrishnan, and P. Narayanan. Deep learning with limited numerical precision. In F. Bach and D. Blei, editors, *Proceedings of the 32nd*

International Conference on Machine Learning, volume 37 of *Proceedings of Machine Learning Research*, pages 1737–1746, Lille, France, 07–09 Jul 2015. PMLR. URL <https://proceedings.mlr.press/v37/gupta15.html>.

- D. Hampel and R. O. Winder. Threshold logic. *IEEE Spectrum*, 8(5):32–39, 1971.
- S. Han, H. Mao, and W. J. Dally. Deep compression: Compressing deep neural networks with pruning, trained quantization and Huffman coding. *arXiv:1510.00149*, 2015. doi: 10.48550/ARXIV.1510.00149. URL <https://arxiv.org/abs/1510.00149>.
- D. O. Hebb. *The Organization of Behavior: A Neuropsychological Theory*. Psychology press, 2005.
- K. Helwegen, J. Widdicombe, L. Geiger, Z. Liu, K.-T. Cheng, and R. Nusselder. Latent weights do not exist: Rethinking binarized neural network optimization. *33rd Conference on Neural Information Processing Systems (NeurIPS 2019)*, 2019. URL <https://arxiv.org/abs/1906.02107>.
- M. Horowitz. 1.1 computing’s energy problem (and what we can do about it). In *2014 IEEE International Solid-State Circuits Conference Digest of Technical Papers (ISSCC)*, pages 10–14, 2014. doi: 10.1109/ISSCC.2014.6757323.
- A. G. Howard, M. Zhu, B. Chen, D. Kalenichenko, W. Wang, T. Weyand, M. Andreetto, and H. Adam. Mobilenets: Efficient convolutional neural networks for mobile vision applications. *arXiv preprint arXiv:1704.04861*, 2017.
- C.-W. Huang, T.-W. Chen, and J.-D. Huang. All-you-can-fit 8-bit flexible floating-point format for accurate and memory-efficient inference of deep neural networks. *arXiv:2104.07329*, 2021.
- I. Hubara, M. Courbariaux, D. Soudry, R. El-Yaniv, and Y. Bengio. Binarized neural networks. In *Advances in neural information processing systems*, pages 4107–4115, 2016.
- I. Hubara, M. Courbariaux, D. Soudry, R. El-Yaniv, and Y. Bengio. Quantized neural networks: Training neural networks with low precision weights and activations. *The Journal of Machine Learning Research*, 18(1):6869–6898, 2017.
- R. Ito and T. Saito. Dynamic binary neural networks and evolutionary learning. In *The 2010 International Joint Conference on Neural Networks*, pages 1–5. IEEE, 2010.
- Q. Jin, J. Ren, R. Zhuang, S. Hanumante, Z. Li, Z. Chen, Y. Wang, K. Yang, and S. Tulyakov. F8Net: Fixed-point 8-bit only multiplication for network quantization. *arXiv preprint arXiv:2202.05239*, 2021.
- H. Kwon, P. Chatarasi, M. Pellauer, A. Parashar, V. Sarkar, and T. Krishna. Understanding reuse, performance, and hardware cost of dnn dataflow: A data-centric approach. In *Proceedings of the 52nd Annual IEEE/ACM International Symposium on Microarchitecture, MICRO 52*, pages 754–768, New York, NY, USA, 2019. Association for Computing Machinery. ISBN 9781450369381. doi: 10.1145/3352460.3358252. URL <https://doi.org/10.1145/3352460.3358252>.

- I. Lavi, S. Avidan, Y. Singer, and Y. Hel-Or. Proximity preserving binary code using signed graph-cut. In *Proceedings of the AAAI Conference on Artificial Intelligence*, volume 34, pages 4535–4544, 2020.
- Y. LeCun, L. Bottou, Y. Bengio, and P. Haffner. Gradient-based learning applied to document recognition. *Proceedings of the IEEE*, 86(11):2278–2324, 1998.
- H. Liao, J. Tu, J. Xia, H. Liu, X. Zhou, H. Yuan, and Y. Hu. Ascend: a scalable and unified architecture for ubiquitous deep neural network computing : Industry track paper. In *2021 IEEE International Symposium on High-Performance Computer Architecture (HPCA)*, pages 789–801, 2021. doi: 10.1109/HPCA51647.2021.00071.
- C. Liu, W. Ding, X. Xia, B. Zhang, J. Gu, J. Liu, R. Ji, and D. Doermann. Circulant binary convolutional networks: Enhancing the performance of 1-bit dcnn with circulant back propagation. In *Proceedings of the IEEE Conference on Computer Vision and Pattern Recognition*, pages 2691–2699, 2019.
- Z. Liu, B. Wu, W. Luo, X. Yang, W. Liu, and K.-T. Cheng. Bi-real net: Enhancing the performance of 1-bit cnns with improved representational capability and advanced training algorithm. In *Proceedings of the European conference on computer vision (ECCV)*, pages 722–737, 2018. URL <https://github.com/ichakra2/pca-hybrid>.
- Z. Liu, Z. Shen, M. Savvides, and K.-T. Cheng. ReActNet: Towards precise binary neural network with generalized activation functions. In *European Conference on Computer Vision*, pages 143–159, 2020.
- A. K. Maan, D. A. Jayadevi, and A. P. James. A survey of memristive threshold logic circuits. *IEEE Transactions on Neural Networks and Learning Systems*, 28(8): 1734–1746, 2017.
- F. J. MacWilliams and N. J. A. Sloane. *The Theory of Error-Correcting Codes*, volume 16. North-Holland Publishing Company, Amsterdam, 1977. URL www.academia.edu/download/43668701/linear_codes.pdf.
- W. S. McCulloch and W. Pitts. A logical calculus of the ideas immanent in nervous activity. *The Bulletin of Mathematical Biophysics*, 5(4):115–133, 1943.
- G. Morse and K. O. Stanley. Simple evolutionary optimization can rival stochastic gradient descent in neural networks. In *Proceedings of the Genetic and Evolutionary Computation Conference 2016*, pages 477–484, 2016.
- M. Rastegari, V. Ordonez, J. Redmon, and A. Farhadi. XNOR-Net: Imagenet classification using binary convolutional neural networks. In *European Conference on Computer Vision*, pages 525–542. Springer, 2016.
- M. Rutter. An introduction to computing, 2001. URL <https://www.mjr19.org.uk/courses/lect1.pdf>.
- A. Sebastian, M. Le Gallo, R. Khaddam-Aljameh, and E. Eleftheriou. Memory devices and applications for in-memory computing. *Nature Nanotechnology*, 15(7):529–544, 2020.

- K. Simonyan and A. Zisserman. Very deep convolutional networks for large-scale image recognition. *arXiv preprint arXiv:1409.1556*, 2014.
- D. Soudry, I. Hubara, and R. Meir. Expectation backpropagation: Parameter-free training of multilayer neural networks with continuous or discrete weights. In *Advances in Neural Information Processing Systems*, pages 963–971, 2014.
- E. Strubell, A. Ganesh, and A. McCallum. Energy and policy considerations for deep learning in NLP. In *Proceedings of the 57th Annual Meeting of the Association for Computational Linguistics*, pages 3645–3650, Florence, Italy, Jul 2019. Association for Computational Linguistics. doi: 10.18653/v1/P19-1355. URL <https://aclanthology.org/P19-1355>.
- X. Sun, N. Wang, C.-Y. Chen, J. Ni, A. Agrawal, X. Cui, S. Venkataramani, K. E. Maghraoui, V. V. Srinivasan, and K. Gopalakrishnan. Ultra-low precision 4-bit training of deep neural networks. In *Advances in Neural Information Processing Systems 33 pre-proceedings (NeurIPS 2020)*, 2020. URL <https://proceedings.neurips.cc/paper/2020/hash/13b919438259814cd5be8cb45877d577-Abstract.html>.
- V. Sze, Y.-H. Chen, T.-J. Yang, and J. S. Emer. Efficient processing of deep neural networks: A tutorial and survey. *Proc. IEEE*, 105(12):2295–2329, 2017. URL <https://ieeexplore.ieee.org/document/8114708>.
- V. Sze, Y.-H. Chen, T.-J. Yang, and J. S. Emer. Efficient processing of deep neural networks. *Synthesis Lectures on Computer Architecture*, 15(2):1–341, 2020a.
- V. Sze, Y.-H. Chen, T.-J. Yang, and J. S. Emer. How to evaluate deep neural network processors: Tops/w (alone) considered harmful. *IEEE Solid-State Circuits Mag.*, 12(3):28–41, 2020b.
- M. Tan and Q. Le. EfficientNet: Rethinking model scaling for convolutional neural networks. In K. Chaudhuri and R. Salakhutdinov, editors, *Proceedings of the 36th International Conference on Machine Learning*, volume 97 of *Proceedings of Machine Learning Research*, pages 6105–6114. PMLR, 09–15 Jun 2019. URL <https://proceedings.mlr.press/v97/tan19a.html>.
- Y. Umuroglu, N. J. Fraser, G. Gambardella, M. Blott, P. Leong, M. Jahre, and K. Vissers. FINN: A framework for fast, scalable binarized neural network inference. In *Proceedings of the 2017 ACM/SIGDA International Symposium on Field-Programmable Gate Arrays*, pages 65–74, 2017.
- N. Verma, H. Jia, H. Valavi, Y. Tang, M. Ozatay, L.-Y. Chen, B. Zhang, and P. Deaville. In-memory computing: Advances and prospects. *IEEE Solid-State Circuits Mag.*, 11(3):43–55, 2019. doi: 10.1109/MSSC.2019.2922889.
- K. Yamamoto. Learnable companding quantization for accurate low-bit neural networks. *arXiv:2103.07156*, 2021.
- T.-J. Yang, Y.-H. Chen, J. Emer, and V. Sze. A method to estimate the energy consumption of deep neural networks. In *2017 51st Asilomar Conference on Signals, Systems, and Computers*, pages 1916–1920, Oct 2017a. doi: 10.1109/ACSSC.2017.8335698.

- T.-J. Yang, Y.-H. Chen, and V. Sze. Designing energy-efficient convolutional neural networks using energy-aware pruning. In *Proceedings of the IEEE Conference on Computer Vision and Pattern Recognition (CVPR)*, July 2017b.
- X. Yang, M. Gao, Q. Liu, J. Setter, J. Pu, A. Nayak, S. Bell, K. Cao, H. Ha, P. Raina, et al. Interstellar: Using halide’s scheduling language to analyze dnn accelerators. In *Proceedings of the Twenty-Fifth International Conference on Architectural Support for Programming Languages and Operating Systems*, pages 369–383, 2020.
- X. Yang, B. Taylor, A. Wu, Y. Chen, and L. O. Chua. Research progress on memristor: From synapses to computing systems. *IEEE Trans. Circuits Syst. I*, 69(5):1845–1857, May 2022a. ISSN 1558-0806. doi: 10.1109/TCSI.2022.3159153.
- Y. Yang, X. Chi, L. Deng, T. Yan, F. Gao, and G. Li. Towards efficient full 8-bit integer DNN online training on resource-limited devices without batch normalization. *Neurocomputing*, 2022b.
- S. Yu and P.-Y. Chen. Emerging memory technologies: Recent trends and prospects. *IEEE Solid-State Circuits Mag.*, 8(2):43–56, 2016. doi: 10.1109/MSSC.2016.2546199.
- D. Zhang, J. Yang, D. Ye, and G. Hua. Lq-nets: Learned quantization for highly accurate and compact deep neural networks. In *Proceedings of the European Conference on Computer Vision (ECCV)*, September 2018.
- H. Zhang, J. Liu, J. Bai, S. Li, L. Luo, S. Wei, J. Wu, and W. Kang. HD-CIM: Hybrid-device computing-in-memory structure based on mram and sram to reduce weight loading energy of neural networks. *IEEE Trans. Circuits Syst. I*, 69(11):4465–4474, Nov 2022a. ISSN 1558-0806. doi: 10.1109/TCSI.2022.3199440.
- Y. Zhang, Z. Zhang, and L. Lew. PokeBNN: A binary pursuit of lightweight accuracy. In *Proceedings of the IEEE/CVF Conference on Computer Vision and Pattern Recognition*, pages 12475–12485, 2022b.